

AGU

PUBLICATIONS

[*Geophysical Research Letter*]

Supporting Information for

The role of subslab low-velocity anomalies beneath the Nazca Ridge and Iquique Ridge on the Nazca Plate and their possible contribution to the subduction angle

Hwaju Lee¹, YoungHee Kim^{1,2*}, Maximiliano J. Bezada³, Robert W. Clayton⁴

¹Research Center for Deep-Surface Coupling of Earth, Seoul, Republic of Korea

²School of Earth and Environmental Sciences, Seoul National University, Seoul, Republic of Korea

³Department of Earth and Environmental Sciences, University of Minnesota, MN, USA

⁴Division of Geological and Planetary Sciences, California Institute of Technology, Pasadena, CA, USA

*Correspondence to: YoungHee Kim (younghkim@snu.ac.kr)

Contents of this file

Table S1. List of network stations used in this study.

Text S1. Detailed explanations on how we developed the two anisotropy models based SWS observations and brief method of including the models in the inversion.

Figure S1. The distribution of teleseismic events used in this study. The left and right panels show the events within in 30–90° and 120–180° distances, respectively.

Figure S2. L-curve is used to determine the optimum regularization parameters (damping and smoothing). The damping parameter increases from left to right within the same smoothing parameter curve. The blue dot on the red line presents the parameters used in this study.

Figure S3. Synthetic test results for Nazca Ridge region (flat slab).

Figure S4. Synthetic test results for Iquique Ridge region (normal slab).

Figure S5. Normalized hit quality test of rays at different depth slices.

Figure S6. Mapviews of targeted SSLAs and anisotropy models beneath Nazca Ridge and Iquique Ridge.

Figure S7. Comparison of isotropic dV_p/V_p (a–c) and prescribed anisotropy dV_p/V_p (d–f) tomographic images at different depth slices for the Nazca Ridge region.

Figure S8. Comparison of isotropic dV_p/V_p (a–c) and prescribed anisotropy dV_p/V_p (d–f) tomographic images at different depth slices for the Iquique Ridge region.

Figure S9. Quantitative comparisons on the isotropic model (blue) and prescribed-anisotropy model (red). Root-mean-square (RMS) of travel time residuals (second) vs. normalized model norm (%) for the targeted sub-slab low-velocity anomalies for (a) Nazca Ridge at depths of 50–210 km and (b) Iquique Ridge at 250–420 km.

Introduction

This document includes Table S1 to list the seismic network and stations used in this study and Text S1 to explain details on how we 1) develop the anisotropy models based on SWS observations and 2) include them in the tomographic inversion. Figure S1 shows the distribution of the teleseismic events used in the study. Figure S2 shows how we determine the regularization for our tomography. Figures S3, S4, and S5 show the tests carried out to ensure the resolution of our tomographic models. Figure S6 shows the mapviews of targeted SSLAs and anisotropy models. Figures S7 and S8 support Figure 2. Figure S9 shows the quantitative changes in travel-time residual and model norm.

Network code	Data center	Description	# of stations used in the study	Period of data used in the study (year)
C	IRIS (FDSN)	Chilean National Seismic Network	1	2011-2013
CX	GEOFON	Integrated Plate boundary Observatory Chile (IPOC) Seismic Network	12	2007-2013
GT	IRIS (FDSN)	Global Telemetered Seismograph Network (GTSN)	1	2011-2013
TO	IRIS	Tectonic Observatory (PeruSE)	133	2007-2013
YS	IRIS (FDSN)	The life cycle of Andean volcanoes: Combining space-based and field studies (ANDIVOLC)	1	2011-2012
ZD	IRIS	PerU Lithosphere and Slab Experiment (PULSE)	40	2010-2013
ZG	IRIS	Central Andean Uplift and the Geodynamics of the High Topography (CAUGH)	49	2010-2012

Table S1. Station network metadata. Seismic networks used in this study are sorted alphabetically based on the network name. The instrument type of all stations is broadband (BHZ).

Text S1. Development of anisotropy models and

From the observed SWS (Deng et al., 2017; Eakin et al., 2014, 2015; Long et al., 2016; Lynner & Beck, 2020; Polet et al., 2000; Reiss et al., 2018), two pieces of information that we obtained are splitting time and fast polarization direction (FPD). The splitting time can represent the accumulated anisotropy along the ray path. As we hypothetically presumed that the SSLAs come from seismic anisotropy, we assume that the shear wave would have been split while traveling through the low-velocity anomalies (Figure S6). In other words, along the ray path, the mantle is isotropic (no split) except for the volume of low-velocity anomalies found beneath the two ridges. The field of our anisotropy models is designed to reproduce the inferred splitting time at each station above the low-velocity anomalies (Figure 1c). We translated V_S anisotropy (AV_S) from the SWS observation to V_P anisotropy (AV_P) by multiplying the constant of 1.51 to make it usable in our P-wave tomography inversion. The constant value comes from elastic tensors of natural peridotite (Hammond & Toomey, 2003; Kern, 1993) and further details of the conversion can be found in Hammond & Toomey (2003) and Lee et al. (2021). The AV_P is depth-dependent. Simultaneously, we could infer the direction of mantle flow from FPD as the seismically fast direction of A-type olivine fabric aligns with the direction of mantle flow (Anderson, 1989; Hirth & Kohlstedt, 2003; Ismaïl & Mainprice, 1998; Kaminski & Ribe, 2002; Tommasi et al., 1999). From previous studies of SWS (Deng et al., 2017; Eakin et al., 2014, 2015; Long et al., 2016; Lynner & Beck, 2020; Polet et al., 2000; Reiss et al., 2018), we generally find trench-parallel FPD in the northern vicinity where Nazca Ridge subducts at a low angle with some null measurements around the Nazca Ridge subducting area (flat slab subduction) (Figure 1). A transition from trench-perpendicular-to-trench-parallel FPD is observed in the vicinity of Iquique Ridge which subducts at a normal angle (normal-dip subduction) (Figure 1). Accordingly, the seismically fast axis of our anisotropy models is set to reproduce the splitting time and inferred FPD based on SWS observations (Figures 1 and S6). For instance, when a splitting time of 1 s comes from 50–200 km depths of the mantle (i.e., Nazca Ridge case), it gives a 4.5% anisotropic field. In comparison, when a splitting time of 1 s comes from 250–420 km depths, it gives a 4.2% anisotropic field. Depending on the SWS time observed above subducted Nazca Ridge and the volume of SSLAs beneath, the field of anisotropy model laid at depths of 50–200 km varies from 0 to ~11% (Figures S6a and b). Likewise, the field of anisotropy model based on the volume of SSLA at 250–420 km and observed SWS time for the Iquique Ridge varies from 0 to 7% (Figures S6c and d). We note that anisotropy models are placed where the resolution of tomographic models (ray coverage) is acceptable (Figures S5 and S6): the anisotropy models for the Nazca Ridge and the Iquique Ridge are placed inland and within the neritic zone, respectively.

Distribution of teleseismic events used in study

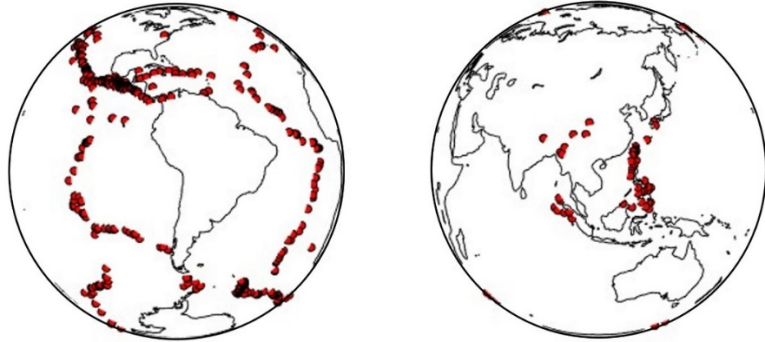


Figure S1. The distribution of teleseismic events used in this study. The left and right panels show the events within in 30–90° and 155–180° distances, respectively.

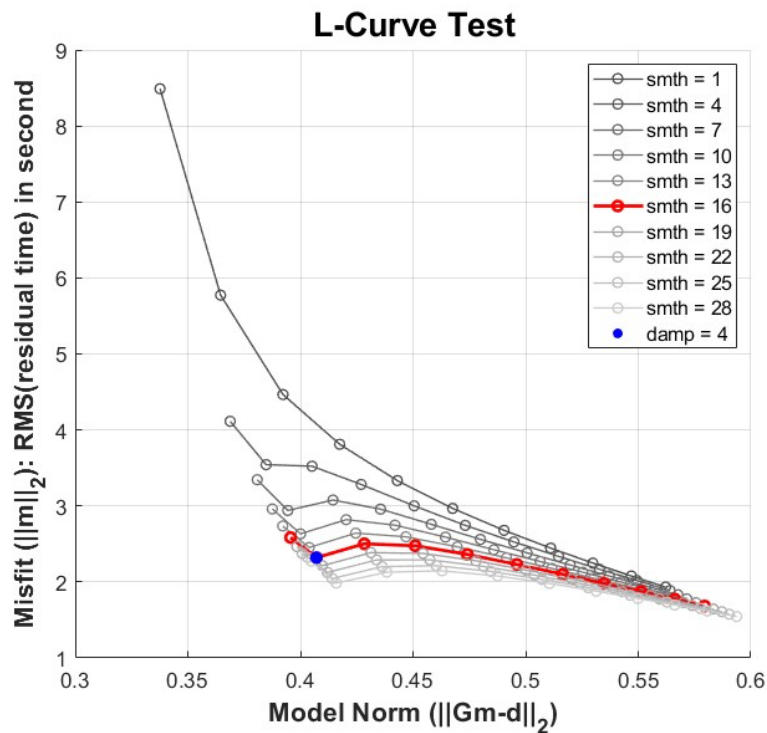


Figure S2. L-curve is used to determine the optimum regularization parameters (damping and smoothing). The damping parameter increases from left to right within the same smoothing parameter curve. The blue dot on the red line presents the parameters used in this study.

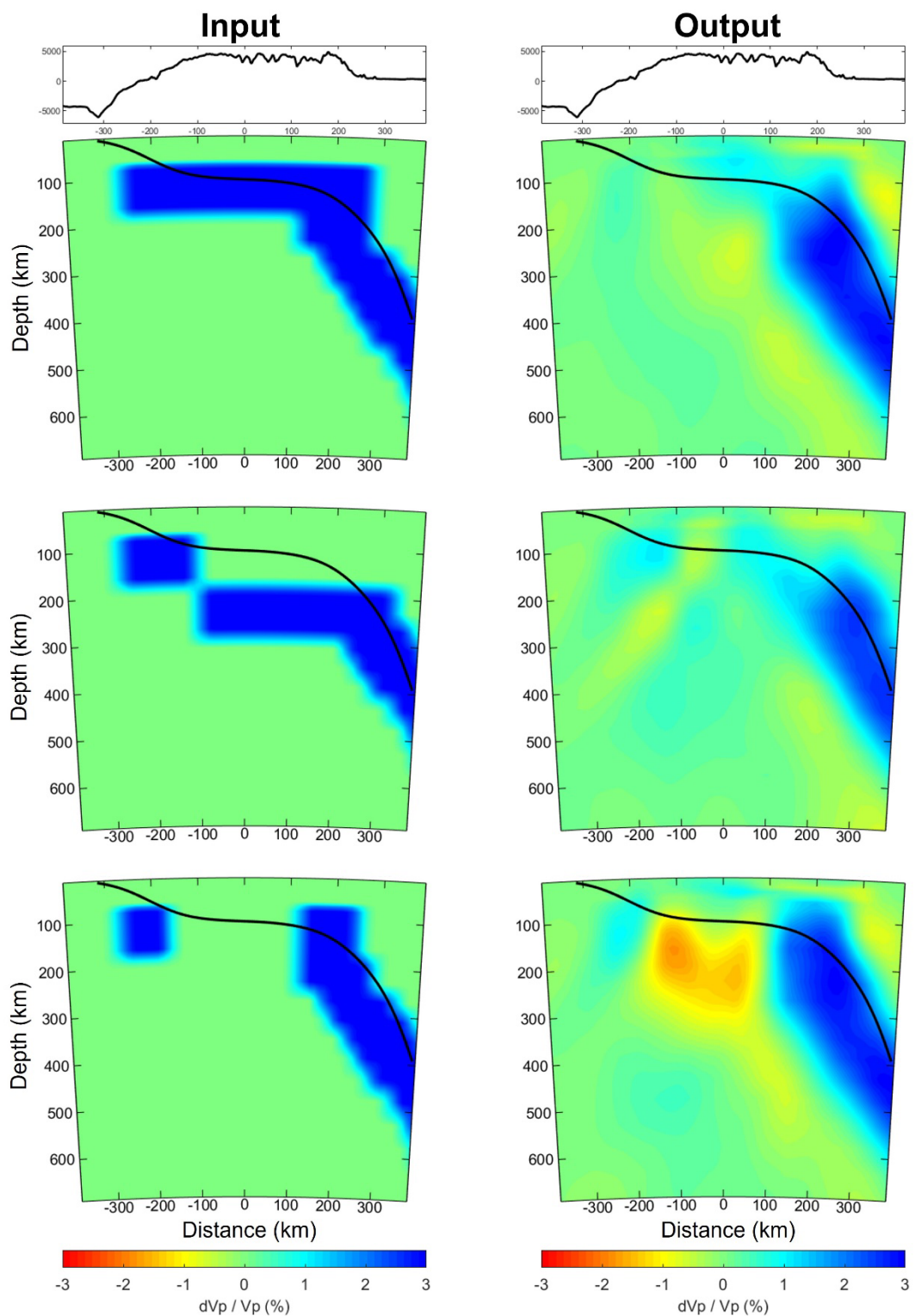


Figure S3. Synthetic test results for Nazca Ridge region (flat slab).

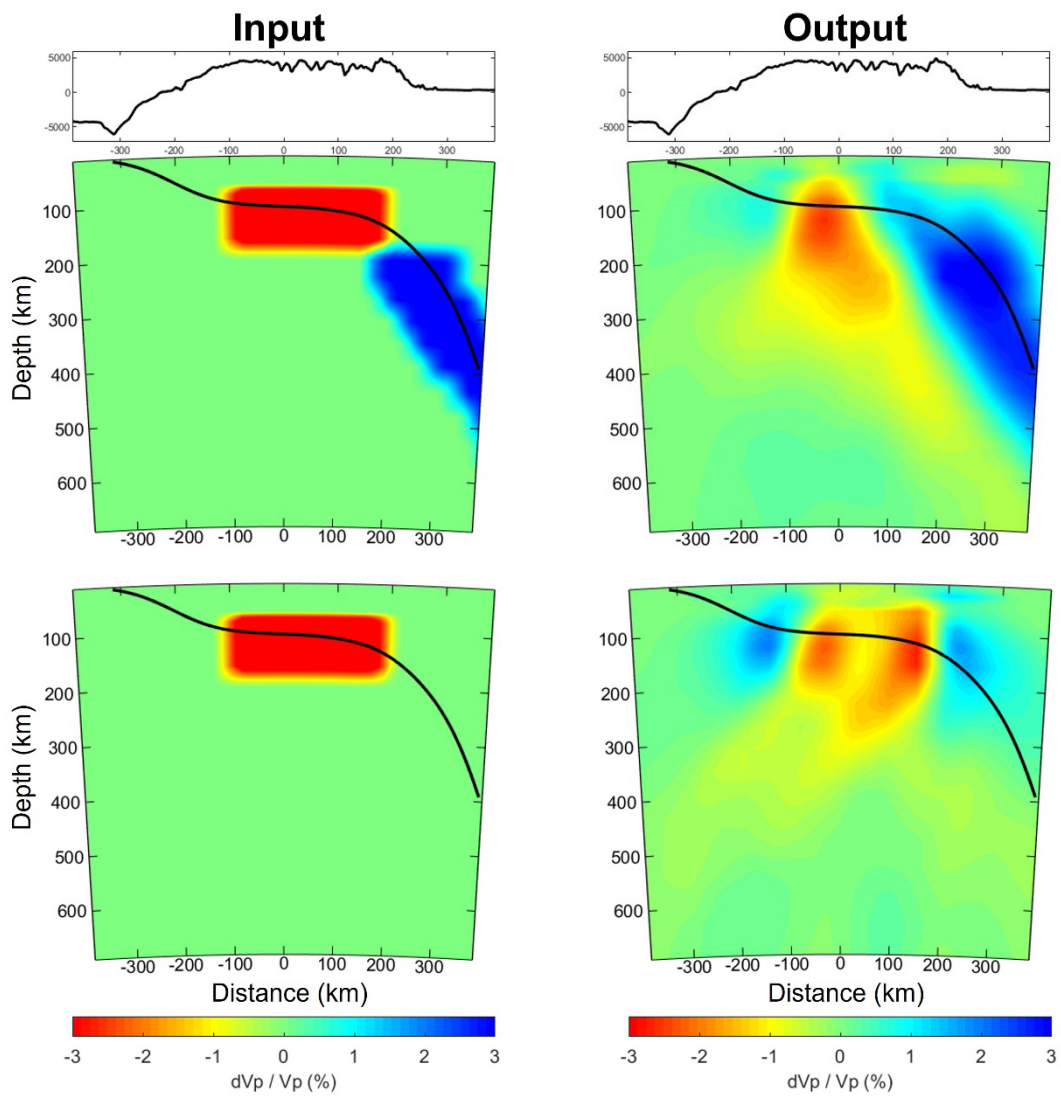


Figure S3. Synthetic test results for Nazca Ridge region (flat slab) (continued).

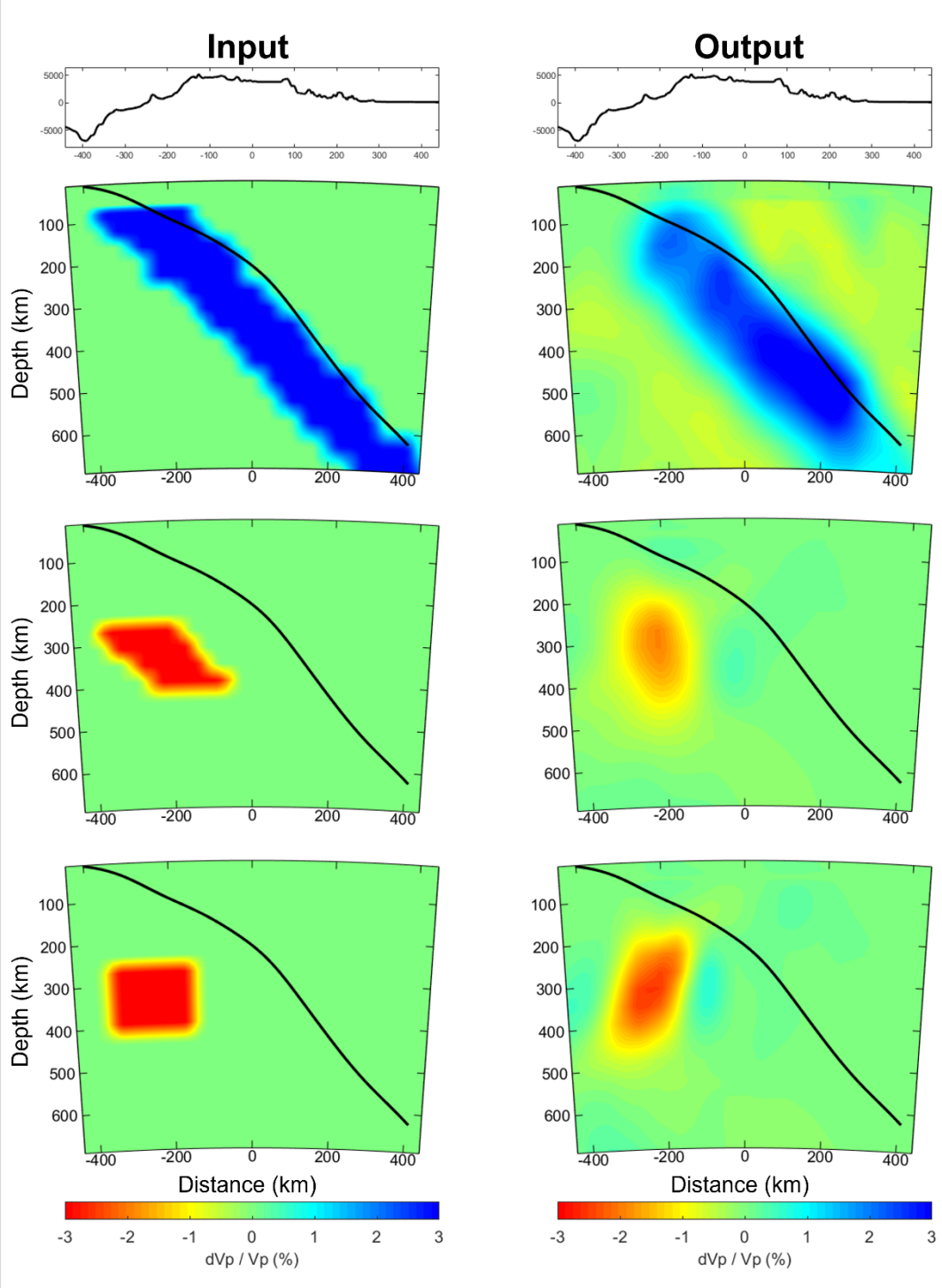


Figure S4. Synthetic test results for Iquique Ridge region (normal slab).

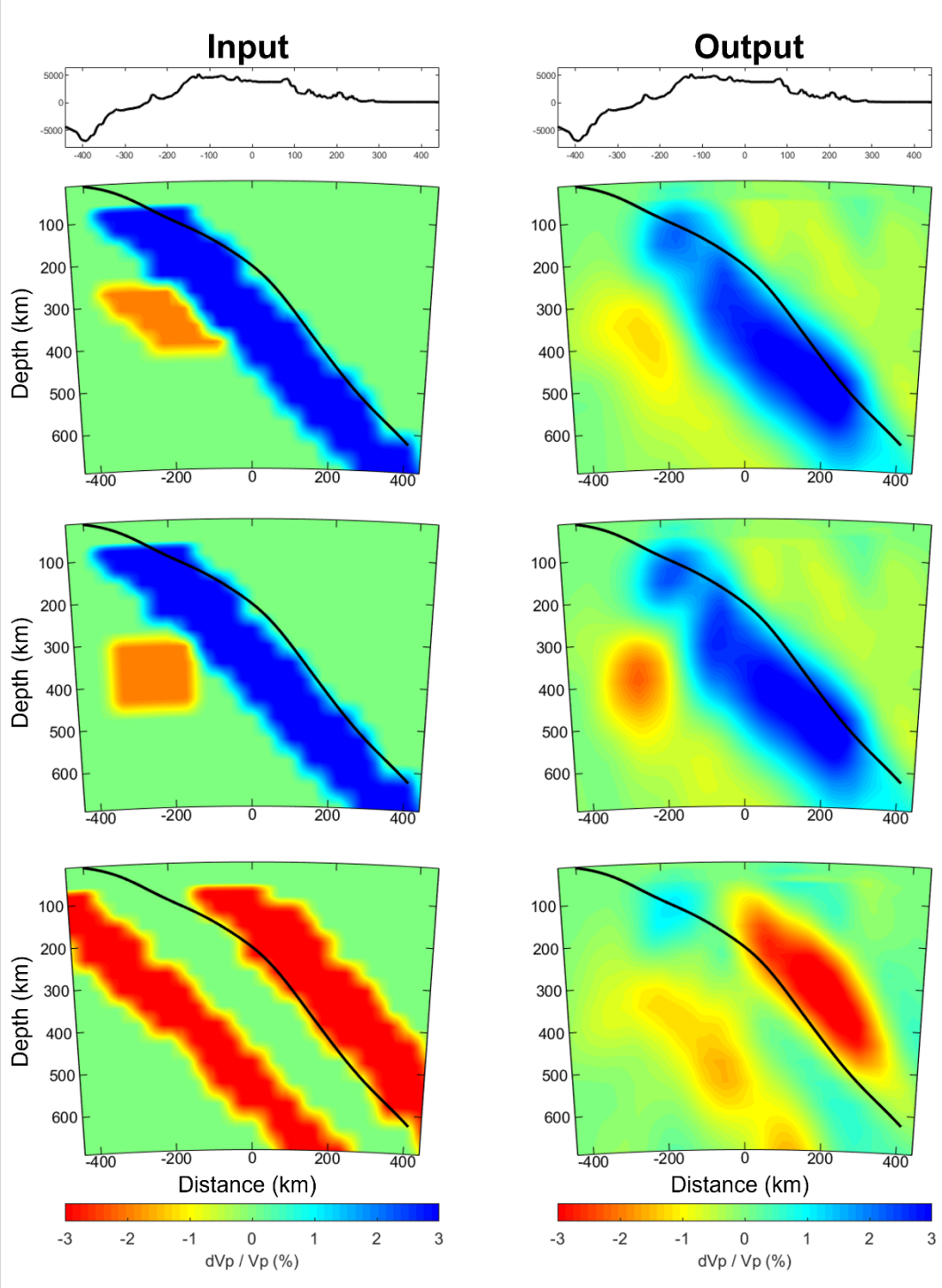


Figure S4. Synthetic test results for Iquique Ridge region (normal slab) (continued).

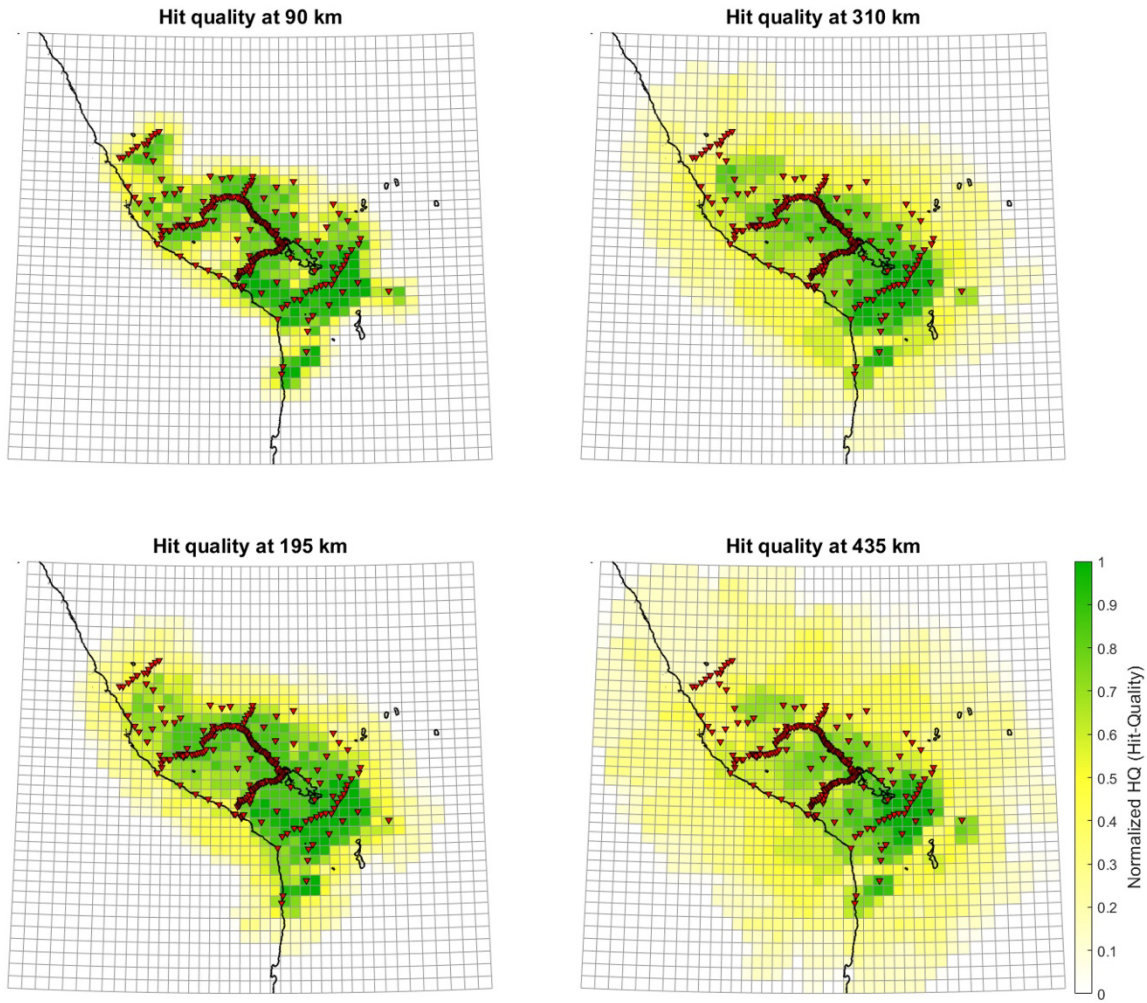


Figure S5. Normalized hit quality test of rays at different depth slices.

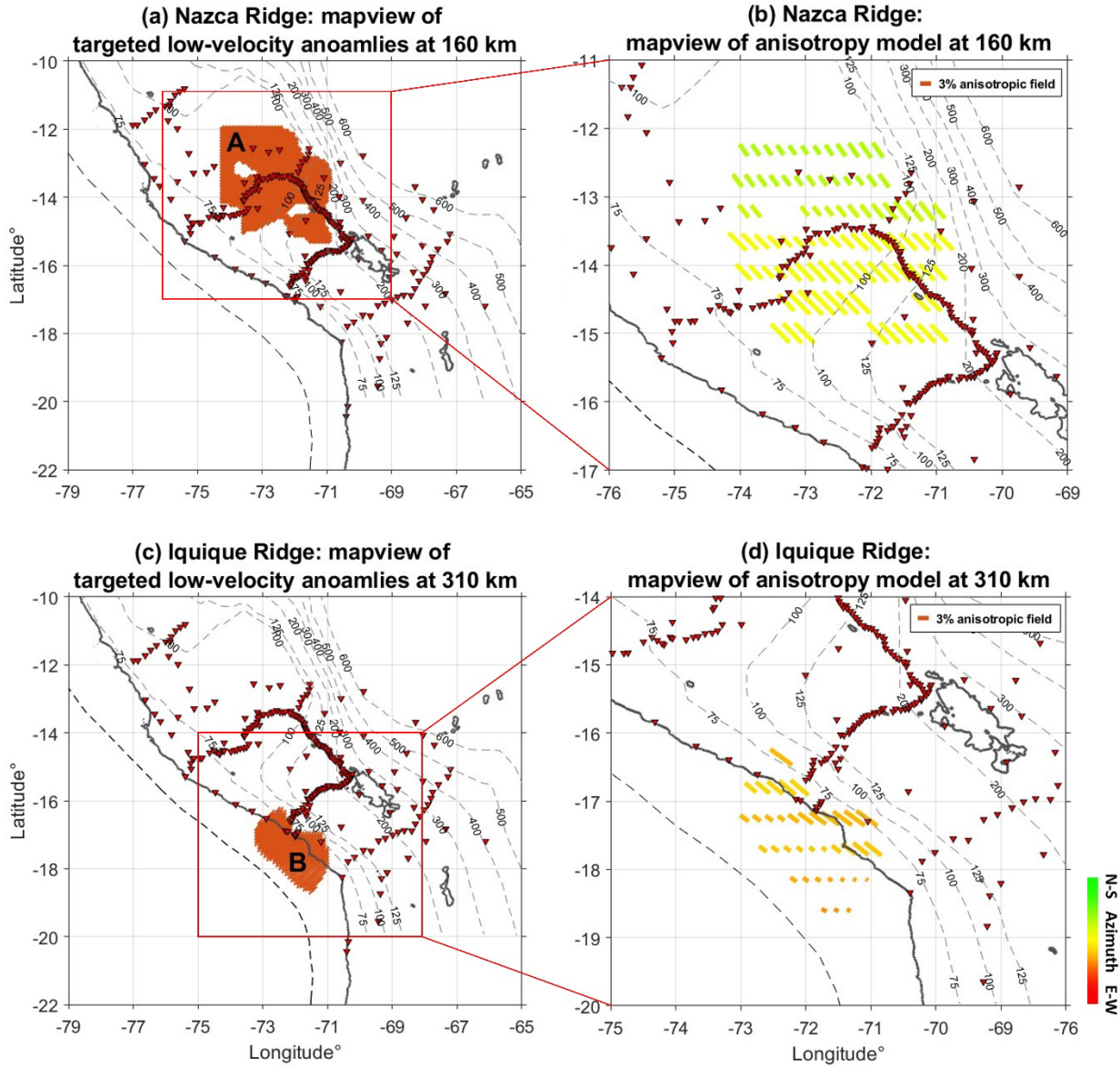


Figure S6. Mapview of targeted sub-slab low-velocity anomalies beneath the (a) Nazca Ridge at 160 km (denoted as ‘A’) and (c) Iquique Ridge at 310 km denoted as ‘B’. Mapivews of prescribed anisotropy models at (b) 160 km beneath the Nazca Ridge and (d) at 310 km beneath the Iquique Ridge. The length of the anisotropy bar represents the strength of anisotropy while the change in its orientation represents azimuth that is color-coded. The red inverted triangles are seismic stations used in this study, and the solid thick grey line is the coastal line. The thick dashed grey line shows the trench while thin dashed grey lines show the iso-depth contours of the subducted Nazca Plate by Scire et al. (2016).

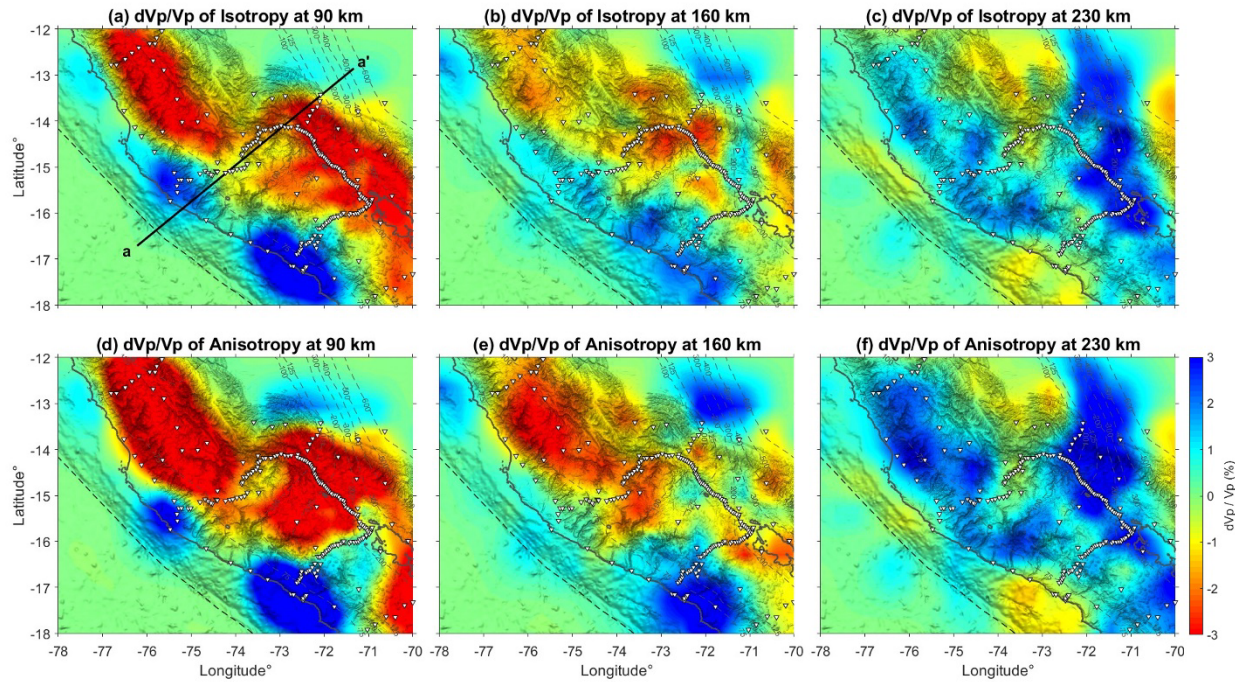


Figure S7. Comparison of isotropic dV_p/V_p (a–c) and prescribed anisotropy dV_p/V_p (d–f) tomographic images at different depth slices for the Nazca Ridge region.

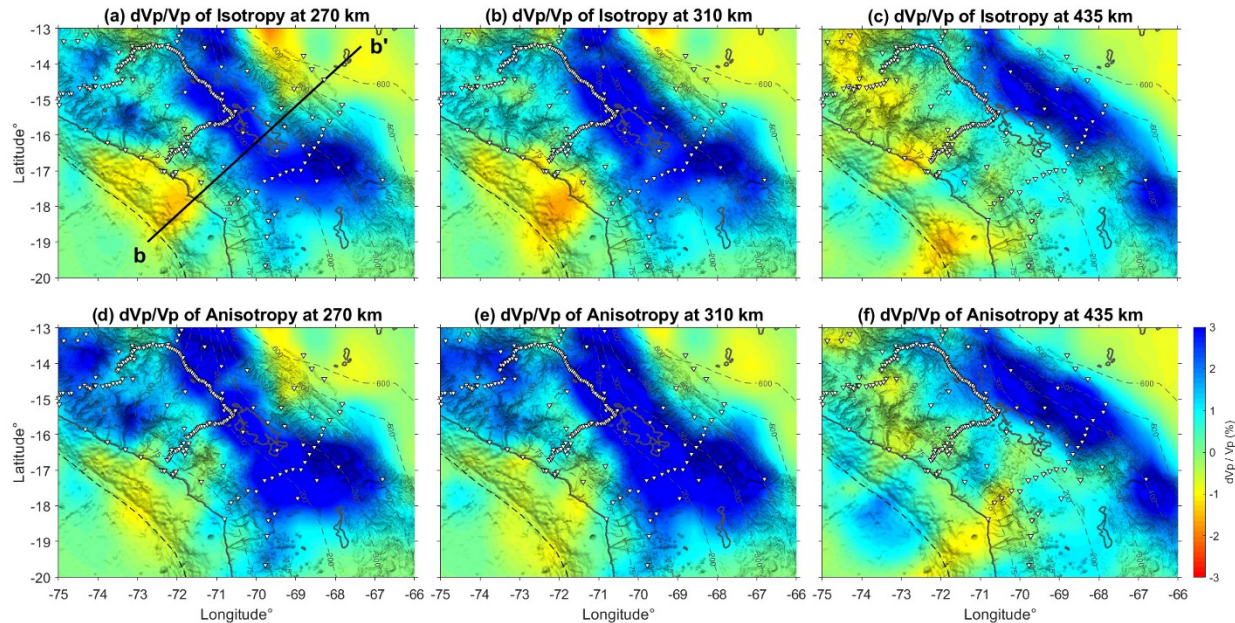


Figure S8. Comparison of isotropic dV_p/V_p (a–c) and prescribed anisotropy dV_p/V_p (d–f) tomographic images at different depth slices for the Iquique Ridge region.

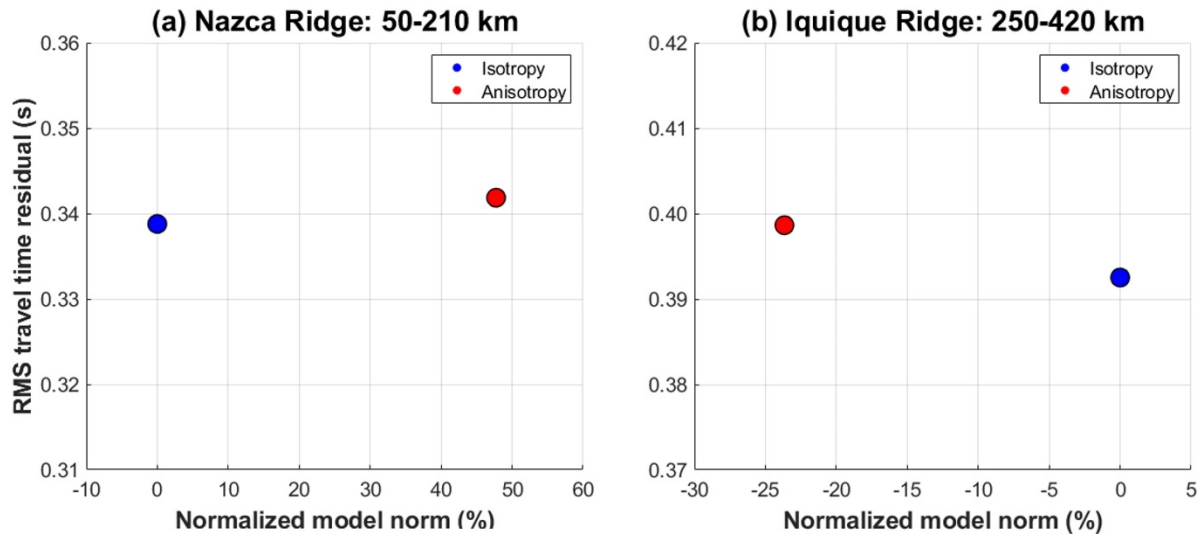


Figure S9. Quantitative comparisons on the isotropic model (blue) and prescribed-anisotropy model (red). Root-mean-square (RMS) of travel time residuals (second) vs. normalized model norm (%) for the targeted sub-slab low-velocity anomalies for (a) Nazca Ridge at depths of 50–210 km and (b) Iquique Ridge at 250–420 km.